




The Rcs System Contributes to the Motility Defects of the Twin-Arginine Translocation System Mutant of Extraintestinal Pathogenic *Escherichia coli*

Te Liu,^a Yuying Liu,^a Zixuan Bu,^a Fan Yin,^a Yongqing Zhang,^a Jinjin Liu,^f Shaowen Li,^a Chen Tan,^{a,b,c} Xiabing Chen,^e Lu Li,^{a,b,c}  Rui Zhou,^{a,b,c,d} Qi Huang^{a,b,c}

^aState Key Laboratory of Agricultural Microbiology, College of Veterinary Medicine, Huazhong Agricultural University, Wuhan, China

^bCooperative Innovation Center for Sustainable Pig Production, Wuhan, China

^cInternational Research Center for Animal Disease, Ministry of Science and Technology, Wuhan, China

^dThe HZAU-HVSEN Institute, Wuhan, China

^eInstitute of Animal Husbandry and Veterinary Science, Wuhan Academy of Agricultural Science and Technology, Wuhan, China

^fWuhan Keqian Biology Co., Ltd., Wuhan, China

Te Liu, Yuying Liu, and Zixuan Bu contributed equally to this article. Author order was determined in order of increasing seniority.

ABSTRACT Flagellum-mediated bacterial motility is important for bacteria to take up nutrients, adapt to environmental changes, and establish infection. The twin-arginine translocation system (Tat) is an important protein export system, playing a critical role in bacterial physiology and pathogenesis. It has been observed for a long time that the Tat system is critical for bacterial motility. However, the underlying mechanism remains unrevealed. In this study, a comparative transcriptomics analysis was performed with extraintestinal pathogenic *Escherichia coli* (ExPEC), which identified a considerable number of genes differentially expressed when the Tat system was disrupted. Among them, a large proportion of flagellar biosynthesis genes showed downregulation, indicating that transcription regulation plays an important role in mediating the motility defects. We further identified three Tat substrate proteins, MdoD, AmiA, and AmiC, that were responsible for the nonmotile phenotype. The Rcs system was deleted in the Δtat , the $\Delta mdoD$, and the $\Delta amiA\Delta amiC$ strains, which restored the motility of $\Delta mdoD$ and partially restored the motility of Δtat and $\Delta amiA\Delta amiC$. The flagella were also observed in all of the $\Delta tat\Delta rcsDB$, $\Delta mdoD\Delta rcsDB$, and $\Delta amiA\Delta amiC\Delta rcsDB$ strains, but not in the Δtat , $\Delta mdoD$, and $\Delta amiA\Delta amiC$ strains, by using transmission electron microscopy. Quantitative reverse transcription-PCR data revealed that the regulons of the Rcs system displayed differential expression in the *tat* mutant, indicating that the Rcs signaling was activated. Our results suggest that the Rcs system plays an important role in mediating the motility defects of the *tat* mutant of ExPEC.

IMPORTANCE The Tat system is an important protein export system critical for bacterial physiology and pathogenesis. It has been observed for a long time that the Tat system is critical for bacterial motility. However, the underlying mechanism remains unrevealed. In this study, we combine transcriptomics analysis and bacterial genetics, which reveal that transcription regulation plays an important role in mediating the motility defects of the *tat* mutant of extraintestinal pathogenic *Escherichia coli*. The Tat substrate proteins responsible for the motility defects are identified. We further show that the Rcs system contributes to the motility suppression. We for the first time reveal the link between the Tat system and bacterial motility, which is important for understanding the physiological functions of the Tat system.

KEYWORDS twin-arginine translocation system, motility, flagella, Rcs system, transcription regulation, extraintestinal pathogenic *Escherichia coli*

Editor Mohamed Y. El-Naggar, University of Southern California

Copyright © 2022 American Society for Microbiology. All Rights Reserved.

Address correspondence to Qi Huang, qhuang@mail.hzau.edu.cn.

The authors declare no conflict of interest.

Received 12 December 2021

Accepted 18 February 2022

Published 21 March 2022

Bacteria utilize various protein transport and secretion systems to deliver proteins that are originally synthesized in the cytoplasm to the subcellular locations beyond the cytoplasm to exert their destined physiological functions (1–3). In many bacteria, a unique protein export system, the twin-arginine translocation (Tat) system, exists to transport a variety of proteins across the cytoplasmic membrane (4). One of the distinguishing features of the Tat system is that it transports fully folded proteins (5). It was originally discovered as a transport system that was closely related to the export of cofactor-containing proteins (6). However, its pleiotropic roles in bacterial physiology have been revealed subsequently (4, 7). A large proportion of them are related to anaerobic respiration, including dehydrogenases, formate dehydrogenases, dimethyl sulfoxide (DMSO) reductases, trimethylamine N-oxide (TMAO) reductase, nitrate reductase, etc. (8). Moreover, the Tat system has been demonstrated to play important roles in the pathogenesis of some important bacterial pathogens, such as pathogenic *Escherichia coli*, *Salmonella*, *Pseudomonas aeruginosa*, and *Yersinia pseudotuberculosis* (9). In some bacteria, the Tat system is even reported to be essential for viability (10, 11).

Bacterial flagella compose a complex machine that promotes cellular motility, which is important in nutrient acquisition, environmental adaptation, and pathogenesis (12–14). The biogenesis of bacterial flagella is under sophisticated transcriptional control. In *E. coli*, the *flhDC* operon, which is also known as class I genes, encodes the master regulator that initiates the transcription hierarchy. FlhDC activates the expression of class II genes that encode important regulatory proteins as well as structural components of flagella. Class III genes encode proteins needed in late flagellar assembly, including flagellin FlhC. Precise temporal control of flagellar gene expression ensures the production of flagella when needed (15, 16). Apart from this regulatory hierarchy, the expression of bacterial flagellar genes has been reported to be regulated in response to external signals. The Rcs system is an important signal transduction system involved in bacterial envelope stress response and virulence regulation (13). It is composed of three core components, RcsC, RcsD, and RcsB, in which RcsC is a transmembrane histidine kinase that is autophosphorylated when the system is activated and passes the phosphate to RcsD then to RcsB (17). RcsB serves as a response regulator to regulate the expression of downstream genes (17). The Rcs signaling system has been revealed to exert an important regulatory function in controlling bacterial motility as a negative regulator of flagellar biosynthesis (18, 19). In addition, the Rcs system has been reported to be involved in the expression of a variety of genes involved in capsule formation, biofilm formation, and type VI secretion in response to stresses such as envelope stresses, outer membrane damage, and peptidoglycan perturbation (13, 17, 20). Another regulation system involved in the regulation of flagellar expression is the CpxAR two-component system, which is composed of the sensor histidine kinase CpxA and the response regulator CpxR. It can be activated in response to bacterial adhesion to abiotic surfaces, leading to downregulation of *flhC* expression in enterohemorrhagic *E. coli* (14). Moreover, appropriate expression of flagellin at different stages of infection has been recently revealed as a new strategy of bacterial pathogenesis (21).

Extraintestinal pathogenic *E. coli* (ExPEC) is an important bacterial pathogen causing a variety of diseases, including urinary tract infection, septicemia, meningitis, and even death in both humans and farm animals (22–24). Our previous study showed that the Tat system is critical for the virulence of extraintestinal pathogenic *E. coli* (ExPEC) and revealed that the disruption of the Tat system caused a significant decrease in bacterial motility as reported in other studies (25–27). However, so far, the underlying mechanism of how the Tat system is involved in the regulation of bacterial motility has not been revealed. In this study, we found that in the ExPEC PCN033 strain, deletion of the Tat system caused drastic downregulated expression of flagellar biosynthesis genes. The Tat substrate proteins were further identified that were responsible for the motility defects. We further showed that the Rcs system was a key player that mediates the regulation of motility by the Tat system. Our study for the first time unraveled the link between the Tat system and bacterial motility.

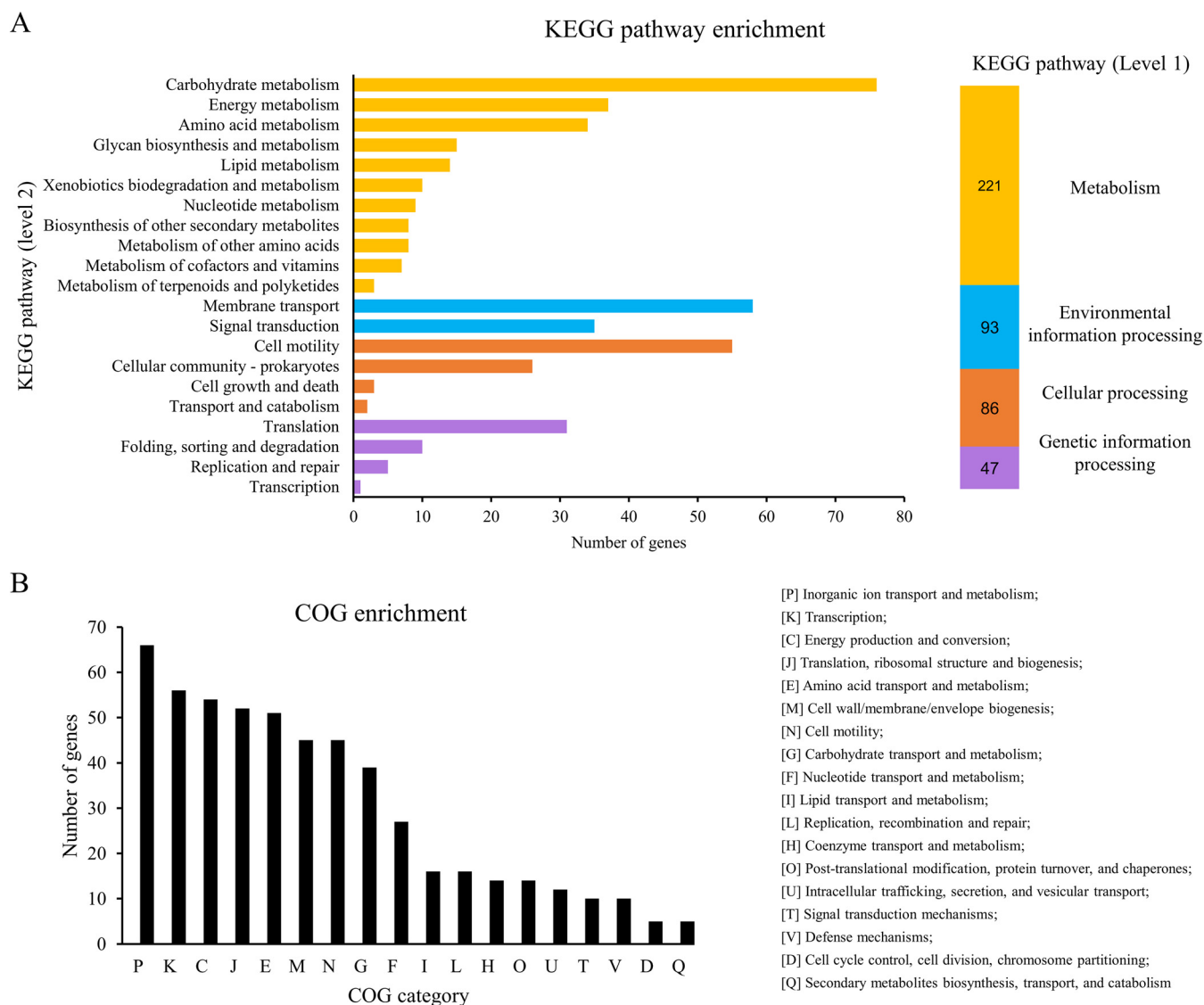


FIG 1 Differentially expressed genes (Δtat versus WT). (A) KEGG pathway enrichment of the differentially expressed genes. The differentially expressed genes were analyzed by using the BlastKOALA tool (<https://www.kegg.jp/blastkoala/>) to assign K numbers which were then used for pathway enrichment by using KEGG Mapper (<https://www.genome.jp/kegg/mapper/search.html>). The numbers inside the vertical bars are the total numbers of genes belonging to each level 2 KEGG pathway. (B) COG enrichment of the differentially expressed genes. COG enrichment was performed with the EggNOG v5.0 database (<http://eggno5.embl.de/#/app/home>).

RESULTS

Deletion of the Tat system causes significant alteration in gene expression. The Tat system has been reported to be involved in a variety of bacterial physiological processes (8). To investigate the influence of the Tat system on gene expression of ExPEC, the transcriptome profiles were compared between ExPEC PCN033 strain (wild type [WT]) and the Tat system-deleted strain (Δtat) by using mRNA sequencing (mRNA-seq). A total of 720 genes were differentially expressed in the Δtat compared with the WT strain [$|\log_2(\text{fold change})| > 1$, $P < 0.05$], among which 508 genes were upregulated and 212 genes were downregulated, indicating an extensive influence on gene expression due to deletion of the Tat system (see Table S1 in the supplemental material). The KEGG database was then used to perform pathway enrichment analysis. As shown in Fig. 1A, metabolism represented the most enriched level 1 KEGG pathways, in which carbohydrate metabolism, membrane transport, and cell motility were the most enriched level 2 KEGG pathways among the differentially expressed genes. Clusters of orthologous groups (COG) enrichment analysis revealed that the differentially expressed genes belonged to a variety of functional categories

TABLE 1 Partial differentially expressed genes in Δ *tat*

No.	Gene ID	Fold change (Δ <i>tat</i> /WT)	P value	FDR	Gene name	Description	Function
1	PPECC33_RS16300	115.360	3.15E-33	3.17E-31	<i>kpsT</i>	ABC transporter ATP-binding protein	Capsular polysaccharide biosynthesis
2	PPECC33_RS16295	40.224	4.71E-70	3.48E-67		HAD-IA family hydrolase	
3	PPECC33_RS16305	36.504	5.56E-40	8.21E-38	<i>kpsM</i>	ABC transporter permease	
4	PPECC33_RS16290	31.779	2.63E-49	7.46E-47		Hypothetical protein	
5	PPECC33_RS16280	17.388	1.96E-20	1.06E-18		Hypothetical protein	
6	PPECC33_RS16275	16.912	5.47E-35	6.21E-33		Nucleotidyltransferase family protein	
7	PPECC33_RS16245	16.912	2.53E-42	4.66E-40	<i>kpsF</i>	KpsF/GutQ family sugar-phosphate isomerase	
8	PPECC33_RS16285	11.472	3.79E-29	3.11E-27		Glycosyltransferase family 2 protein	
9	PPECC33_RS16250	11.314	1.69E-30	1.47E-28	<i>kpsE</i>	Capsule polysaccharide transporter	
10	PPECC33_RS16255	10.056	3.08E-30	2.62E-28	<i>kpsD</i>	Polysaccharide biosynthesis/export family protein	
11	PPECC33_RS16270	8.754	9.30E-19	4.48E-17	<i>kpsS</i>	Capsular biosynthesis protein	Stress response
12	PPECC33_RS16265	7.945	4.89E-31	4.42E-29	<i>kpsC</i>	Capsular polysaccharide biosynthesis protein	
13	PPECC33_RS16260	6.364	4.14E-20	2.21E-18	<i>kpsU</i>	3-Deoxy-manno-octulosonate cytidyltransferase	
14	PPECC33_RS10985	2.346	0.000169	0.000959	<i>wzy</i>	O11 family O-antigen polymerase	
15	PPECC33_RS10950	2.293	6.53E-07	6.77E-06	<i>manC</i>	Mannose-1-phosphate guanylyltransferase/mannose-6-phosphate isomerase	
16	PPECC33_RS10940	2.219	9.50E-08	1.19E-06	<i>cpsG</i>	Colanic acid biosynthesis phosphomannomutase CpsG	
17	PPECC33_RS10945	2.071	1.23E-05	9.69E-05	<i>wcaE</i>	Glycosyltransferase	
18	PPECC33_RS08185	17.509	9.76E-06	7.82E-05	<i>ydeO</i>	Acid stress response transcriptional regulator YdeO	
19	PPECC33_RS07220	5.315	0.000105	0.00064	<i>yciH</i>	Stress response translation initiation inhibitor YciH	
20	PPECC33_RS08195	3.837	2.65E-07	3.01E-06	<i>ydeP</i>	Acid resistance putative oxidoreductase YdeP	
21	PPECC33_RS12175	2.621	1.99E-09	3.33E-08	<i>elaB</i>	Stress response protein ElaB	
22	PPECC33_RS17710	2.549	3.38E-12	8.26E-11	<i>yhcN</i>	Peroxide/acid stress response protein YhcN	
23	PPECC33_RS16005	2.445	1.14E-06	1.12E-05	<i>yggT</i>	Osmotic shock tolerance protein YggT	
24	PPECC33_RS05995	2.219	1.08E-05	8.59E-05	<i>bhsA</i>	Multiple stress resistance protein BhsA	
25	PPECC33_RS22830	105.420	1.41E-09	2.47E-08	<i>ghoT</i>	Type V toxin-antitoxin system toxin GhoT	Toxin-antitoxin system
26	PPECC33_RS22825	22.785	3.52E-06	3.12E-05	<i>ghoS</i>	Type V toxin-antitoxin system endoribonuclease antitoxin GhoS	
27	PPECC33_RS01555	5.657	0.00019	0.001056	<i>yafO</i>	Type II toxin-antitoxin system mRNA interferase toxin YafO	
28	PPECC33_RS03050	3.655	0.009247	0.028521	<i>hokE</i>	Type I toxin-antitoxin system toxin HokE	
29	PPECC33_RS01550	2.395	0.004016	0.014354	<i>yafN</i>	Type I toxin-antitoxin system antitoxin YafN	
30	PPECC33_RS24555	2.238	0.002638	0.010115	<i>lsoB</i>	Type II toxin-antitoxin system antitoxin LsoB	
31	PPECC33_RS07745	0.363	1.37E-08	2.03E-07	<i>hokB</i>	Type I toxin-antitoxin system toxin HokB	
32	PPECC33_RS24945	0.409	8.06E-07	8.20E-06		Type I toxin-antitoxin system Hok family toxin	
33	PPECC33_RS06820	0.432	6.95E-06	5.78E-05	<i>hokD</i>	Type I toxin-antitoxin system toxin HokD	
34	PPECC33_RS00080	0.473	5.55E-07	5.87E-06	<i>mokC</i>	Type I toxin-antitoxin system toxin MokC	
35	PPECC33_RS00280	0.480	0.001035	0.004596		Type II toxin-antitoxin system CcdA family antitoxin	
36	PPECC33_RS27840	0.490	0.01337	0.038627		Type I toxin-antitoxin system toxin Ldr family protein	

(Fig. 1B). Specifically, in the Δ *tat* strain, we found that the genes involved in the biosynthesis of polysialic acid, including the *kpsMT* and *kpsFEDUCS* operons, and the genes involved in the biosynthesis of colonic acid, including *manB* and *manC*, were significantly upregulated (Table 1), indicating that the capsule biosynthesis-related pathway was activated when the Tat system was disrupted. Several stress response genes, including *ydeO* (28), *yciH* (29), *ydeP* (30), *elaB* (31), *yhcN* (32), *yggT* (33), and *bhsA* (34), were also upregulated in the Δ *tat* strain (Table 1). Moreover, we noticed that 12 genes belonging to the toxin-antitoxin systems were differentially expressed, among which 6 genes were upregulated and 6 were downregulated (Table 1). These data suggest that deletion of the Tat system caused substantial changes in gene expression.

Deletion of the Tat system disturbs the expression of flagellar biosynthesis genes. As we reported previously, the deletion of the Tat system in the ExPEC PCN033 strain led to severe defects in motility (Fig. 2A and reference 25). Also, according to the

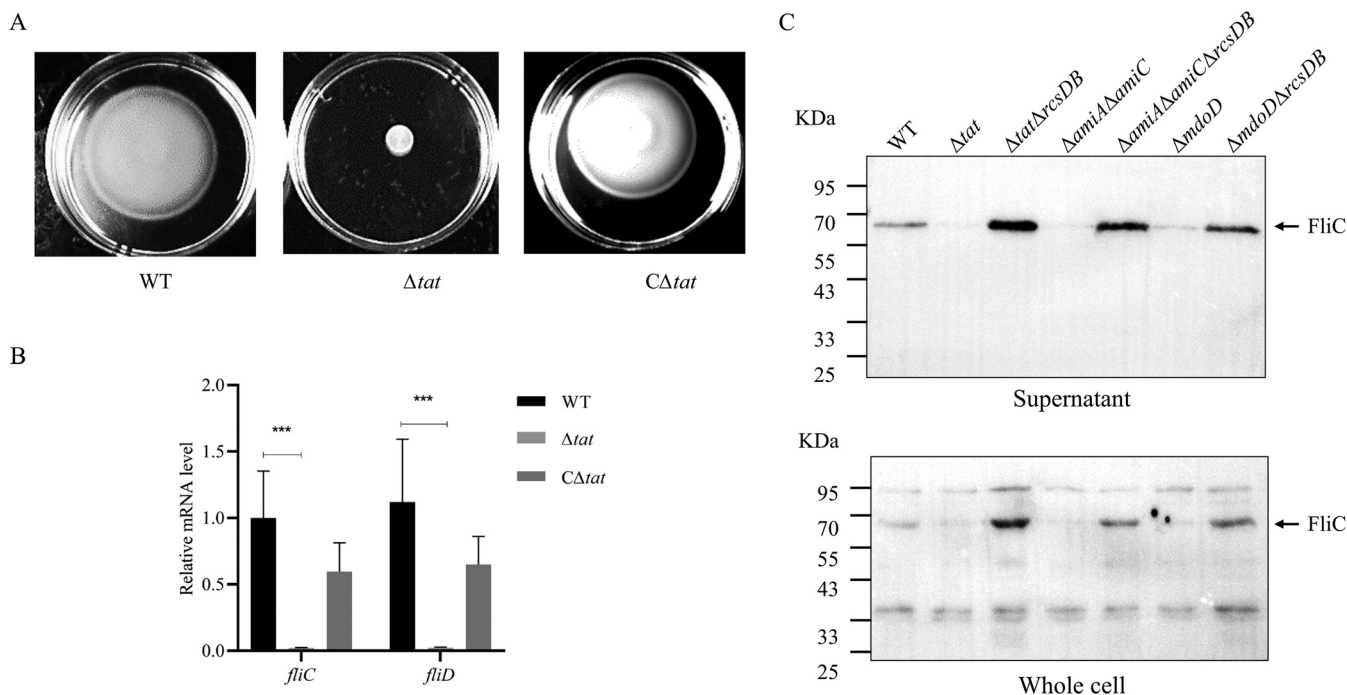


FIG 2 Disruption of the Tat system interferes with the expression of the flagellar biosynthesis genes. (A) In the swimming assay, 5 μ L of cells of each indicated strain at the mid-log phase were spotted onto the swimming plate (tryptone, 10 g/L; yeast, 5 g/L; NaCl, 10 g/L; agar, 0.2%), which was dried at room temperature for 5 min followed by incubation at 37°C for 7 h. The $C\Delta tat$ strain is the Δtat strain harboring a plasmid expressing *tatABC* in *trans*. The assay was performed in triplicate, and the data shown are representative. (B) RT-qPCR analysis. Total RNA was extracted from cells of each indicated strain grown to the mid-log phase. Genomic DNA was removed, and cDNA was synthesized, which was used as the template for qPCR with a QuantStudio 6 Flex fluorescence quantitative PCR instrument. The expression level of the tested gene was calculated using the $2^{-\Delta\Delta CT}$ method and normalized to the housekeeping gene *gapA*. Data are displayed as the geometric mean \pm standard error of the mean (SEM). Statistical significance between the two groups was analyzed using Student's *t* test. ***, $P < 0.001$. (C) Analysis of flagellin production. Cells of each indicated strain were grown to the mid-log phase in LB at 37°C with shaking. The culture was centrifuged, and the same amount of culture supernatant was collected and concentrated by ultracentrifugation. The same number of bacterial cells was harvested, resuspended in PBS, and lysed by sonication, and these were the whole-cell samples. Samples were normalized and subjected to SDS-PAGE followed by Western blotting using anti-FliC antibody (cat. no. ab93713; Abcam).

results of the above KEGG pathway enrichment analysis, cell motility is one of the most influenced pathways in the Δtat strain. Among the first 30 genes with the most down-regulated expression, 11 were directly related to bacterial flagellar biosynthesis, including *fliC* and *fliD*, which encode the flagellin and the flagellar cap protein, respectively (Table 2). Real-time quantitative PCR (RT-qPCR) was performed, which confirmed that the expression levels *fliC* and *fliD* were significantly lower in the Δtat strain than in the WT strain (Fig. 2B). Results of Western blot analysis using anti-FliC antibody also showed a significantly lower level of FliC production in the Δtat strain (Fig. 2C). Therefore, the above-described results suggest that disruption of the Tat system interfered with the expression of flagellar biosynthesis genes.

Tat substrates MdoD, AmiA, and AmiC are responsible for motility defects. To determine which Tat substrate was responsible for the loss of motility of the ExPEC Δtat strain, a motility assay using soft agar was performed with the 20 Tat substrate-related mutant strains, which were constructed in our previous study (25). AmiA and AmiC are both Tat substrates and have overlapping functions. Therefore, a double deletion mutant, $\Delta amiA\Delta amiC$, was constructed and tested (35). As shown in Fig. 3, apart from the Δtat and $\Delta amiA\Delta amiC$ strains, which have been previously shown as motility defective (25), $\Delta mdoD$ also showed significantly compromised motility. In *trans* expression of MdoD in $\Delta mdoD$ from the pHSG396-*Apra*-MdoD plasmid and AmiA and AmiC in $\Delta amiA\Delta amiC$ from the pHSG396-*Apra*-AmiA/AmiC plasmid restored motility (Fig. 3B). As MdoD was a putative Tat substrate and was reported for the first time to be related to bacterial motility, we tested whether the motility phenotype of $\Delta mdoD$ depends on the twin-arginine motif in the N-terminal Tat signal peptide. MdoD^{RR-KK} in which the characteristic twin-arginine (R3 and R4) in its signal peptide was replaced

TABLE 2 The first 30 genes with the most downregulated expression in Δtat

No.	Gene ID	Fold change (Δtat /WT)	P value	FDR	Gene name ^a	Description
1	PPECC33_RS21010	0.001	1.0E-147	4.6E-144	<i>tatA</i>	Sec-independent protein translocase subunit TatA
2	PPECC33_RS21015	0.001	9.10E-66	4.48E-63	<i>tatB</i>	Sec-independent protein translocase subunit TatB
3	PPECC33_RS21020	0.002	4.21E-28	3.27E-26	<i>tatC</i>	Sec-independent protein translocase subunit TatC
4	PPECC33_RS22680	0.011	2.7E-106	6.0E-103	<i>yjcZ</i>	YjcZ-like family protein
5	PPECC33_RS10255	0.024	2.31E-72	2.05E-69	<i>tap</i>	Methyl-accepting chemotaxis protein IV
6	PPECC33_RS10440	0.025	1.48E-39	2.12E-37	<i>fliC*</i>	Flagellin FliC
7	PPECC33_RS10260	0.027	1.73E-41	2.85E-39	<i>tar</i>	Methyl-accepting chemotaxis protein II
8	PPECC33_RS06330	0.033	3.33E-83	4.91E-80	<i>ycgR*</i>	Flagellar brake protein
9	PPECC33_RS12795	0.033	1.38E-48	3.59E-46	<i>flxA</i>	FlxA-like family protein
10	PPECC33_RS10270	0.036	3.73E-43	8.26E-41	<i>cheA</i>	Chemotaxis protein CheA
11	PPECC33_RS10245	0.040	3.04E-58	1.12E-55	<i>cheB</i>	Protein-glutamate methyltransferase/protein glutamine deamidase
12	PPECC33_RS10445	0.045	5.80E-38	8.03E-36	<i>fliD*</i>	Flagellar filament capping protein FliD
13	PPECC33_RS10275	0.046	3.14E-66	1.74E-63	<i>motB*</i>	Flagellar motor protein MotB
14	PPECC33_RS10240	0.049	6.55E-53	2.23E-50	<i>cheY</i>	Chemotaxis response regulator CheY
15	PPECC33_RS10235	0.051	2.01E-78	2.23E-75	<i>cheZ</i>	Protein phosphatase CheZ
16	PPECC33_RS10250	0.051	4.46E-63	1.97E-60	<i>cheR</i>	Protein-glutamate O-methyltransferase CheR
17	PPECC33_RS05845	0.054	2.70E-49	7.46E-47	<i>flgK*</i>	Flagellar hook-associated protein FlgK
18	PPECC33_RS24055	0.054	8.65E-53	2.74E-50	<i>yjiH</i>	Nucleoside recognition pore and gate family inner membrane transporter
19	PPECC33_RS05790	0.058	1.33E-59	5.35E-57	<i>flgM*</i>	Anti-sigma-28 factor FlgM
20	PPECC33_RS10280	0.058	1.01E-37	1.36E-35	<i>motA*</i>	Flagellar motor stator protein MotA
21	PPECC33_RS10265	0.061	3.95E-42	7.00E-40	<i>cheW</i>	Chemotaxis protein CheW
22	PPECC33_RS05850	0.066	8.01E-42	1.36E-39	<i>flgL*</i>	Flagellar hook-associated protein FlgL
23	PPECC33_RS20080	0.068	2.30E-33	2.37E-31	<i>uhpT</i>	Hexose-6-phosphate:phosphate antiporter
24	PPECC33_RS19225	0.073	2.41E-40	3.82E-38	<i>pdeH</i>	Cyclic-guanylate-specific phosphodiesterase
25	PPECC33_RS07750	0.075	1.63E-69	1.03E-66	<i>trg</i>	Methyl-accepting chemotaxis protein Trg
26	PPECC33_RS10455	0.090	3.90E-11	8.23E-10	<i>fliT*</i>	Flagella biosynthesis regulatory protein FliT
27	PPECC33_RS10450	0.108	5.03E-24	3.28E-22	<i>fliS*</i>	Flagellar export chaperone FliS
28	PPECC33_RS05785	0.118	1.25E-20	6.93E-19	<i>flgN*</i>	Flagellar biosynthesis chaperone FlgN
29	PPECC33_RS03935	0.135	1.45E-42	2.80E-40	<i>modA</i>	Molybdate ABC transporter substrate-binding protein
30	PPECC33_RS07110	0.137	5.51E-20	2.91E-18	<i>trpE</i>	Anthranilate synthase component I

^aGenes marked with an asterisk (*) are related to flagellar biosynthesis.

with twin-lysine was expressed from the pHSG396-AprA-MdoD^{RR-KK} plasmid in the $\Delta mdoD$ strain. It was shown that producing the wild-type MdoD in $\Delta mdoD$ restored the motility, while the strain producing MdoD^{RR-KK} was still defective in motility. Our data suggest that it is the Tat substrate proteins MdoD, AmiA, and AmiC that are responsible for the motility defects of the *tat* mutant.

Deletion of *rcsDB* can partially restore the motility of the *tat* mutant. MdoD has been reported as a periplasmic protein involved in glycan biosynthesis, and defects in periplasmic glucan synthesis could induce envelope stress (36–38). AmiA and AmiC are two amidases involved in cell wall remodeling, and their deletion results in cell envelope defects (35). Moreover, several envelope stress response systems, such as the Rcs system and the CpxAR system, have been reported as regulators of bacterial flagella (13, 18, 39). Therefore, a hypothesis was proposed that deletion of the Tat system or the Tat substrates may activate envelope stress response systems which may suppress the expression of flagellar biosynthesis genes. Thus, *rcsDB*, which encodes the essential components of the Rcs signaling system, was deleted from the Δtat , $\Delta mdoD$, and $\Delta amiA\Delta amiC$ strains, and bacterial motility was tested. In Fig. 4, it is shown that the disruption of the Rcs system completely restored the motility defects of the $\Delta mdoD$ strain ($P < 0.05$) and can partially rescue the motility of the Δtat strain and $\Delta amiA\Delta amiC$ strain ($P < 0.05$). To test whether the suppressive effect was specific to the Rcs system, another cell envelope stress response system, CpxAR, was deleted in the Δtat strain, which did not rescue the motility phenotype of Δtat (Fig. 4).

Flagella can be observed in the *tat* mutant when Rcs was disrupted. To further confirm that the restored motility phenotype was due to flagellar biosynthesis, transmission electron microscopy analysis was performed to observe bacterial flagella. Consistent

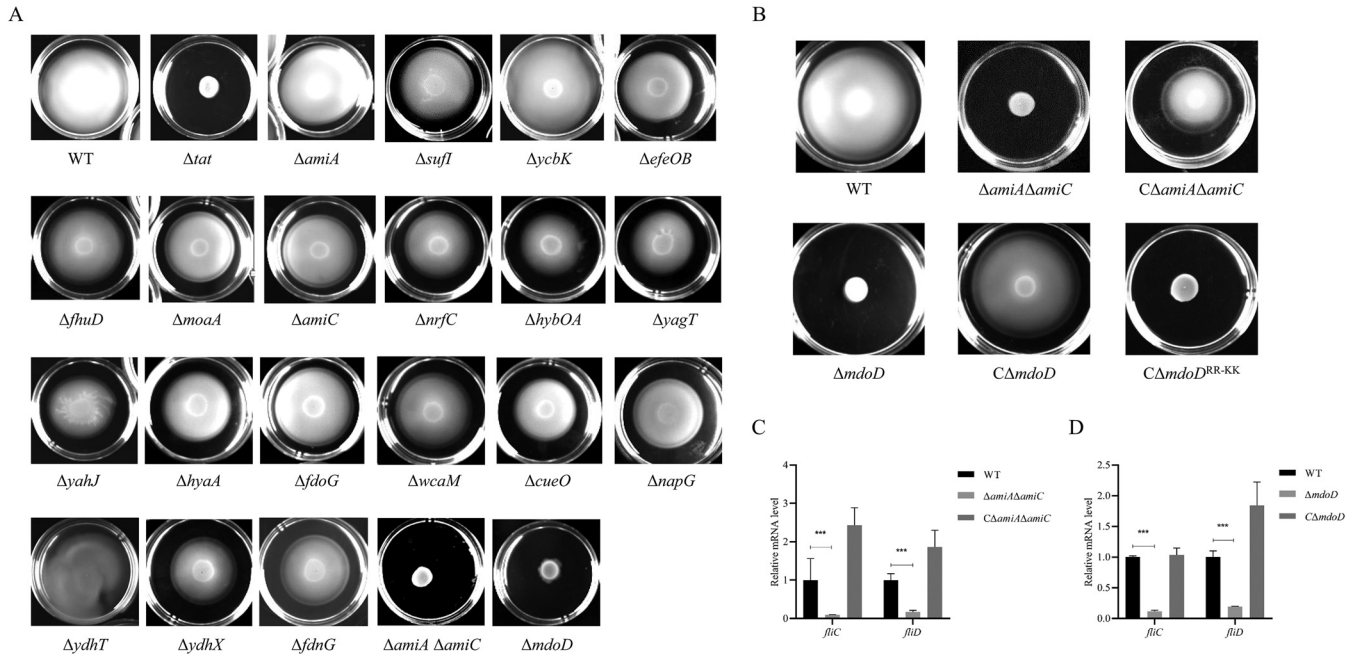


FIG 3 Identification of Tat substrate proteins responsible for loss of motility. (A) For the swimming assay with the Tat substrate-related mutants, 5 μ L of cells of each indicated strain grown to the mid-log phase was spotted onto the swimming plate (tryptone, 10 g/L; yeast, 5 g/L; NaCl, 10 g/L; agar, 0.2%) and was dried at room temperature for 5 min followed by incubation at 37°C for 7 h. The assay was performed in triplicate, and the data shown are representative. (B) Swimming assay with Δ *amiA* Δ *amiC*, Δ *mdoD*, and the strains *in trans* expressing the corresponding proteins. The $C\Delta$ *mdoD* and $C\Delta$ *mdoD*^{RR-KK} strains are the Δ *mdoD* strain encompassing a plasmid encoding the wild type and the mutated MdoD in which the twin-arginine in the signal peptide is replaced with a twin-lysine. $C\Delta$ *amiA* Δ *amiC* is the Δ *amiA* Δ *amiC* strain *in trans* expressing *AmiA* and *AmiC*. (C) and (D) RT-qPCR analysis. Total RNA was extracted from cells of each indicated strain grown to the mid-log phase. Genomic DNA was removed, and cDNA was synthesized and was used as the template for qPCR with a QuantStudio 6 Flex fluorescence quantitative PCR instrument. The expression level of the tested gene was calculated using the $2^{-\Delta\Delta CT}$ method and normalized to the housekeeping gene *gapA*. Data are displayed as the geometric mean \pm SEM. Statistical significance between the two groups was analyzed using Student's *t* test. ***, *P* < 0.001.

with the results of the motility assay, flagella were not seen in Δ *tat*, Δ *modD*, or Δ *amiA* Δ *amiC* but could be observed in the WT, Δ *tat* Δ *rscDB*, Δ *modD* Δ *rscDB*, and Δ *tat* Δ *rscDB* strains, suggesting that the flagellar biosynthesis was recovered when the Rcs system was deleted (Fig. 5). Western blot analysis also showed that FliC expression and secretion were significantly downregulated in Δ *tat*, Δ *modD*, and Δ *amiA* Δ *amiC* but was restored when Rcs was further disrupted (Fig. 2C). It was noticed that the expression of FliC in the *rscDB*-deleted strains was even higher than that in the WT strain. These results suggest that the Rcs system contributes to the disrupted flagellar biosynthesis of the Tat and the Tat substrate mutants.

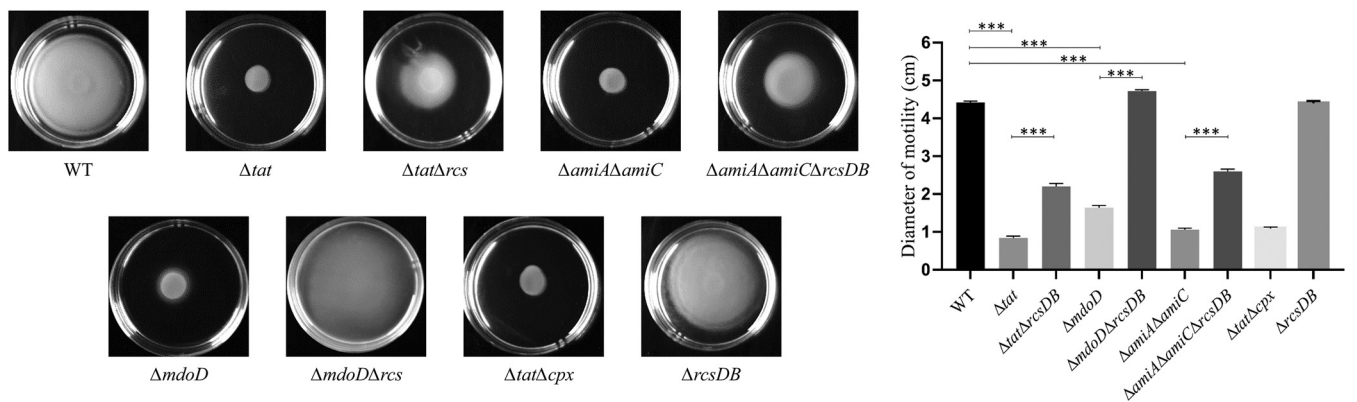


FIG 4 Disruption of the Rcs system restored motility. First, 5 μ L of cells of each indicated strain grown the mid-log phase was spotted onto the swimming plate (tryptone, 10 g/L; yeast, 5 g/L; NaCl, 10 g/L; agar, 0.2%) and was dried at room temperature for 5 min followed by incubation at 37°C for 7 h. The assay was performed in 5 replicates for each strain. The representative image is presented on the left. The swimming diameter is measured and shown as the mean \pm standard deviation on the right. ***, *P* < 0.001.

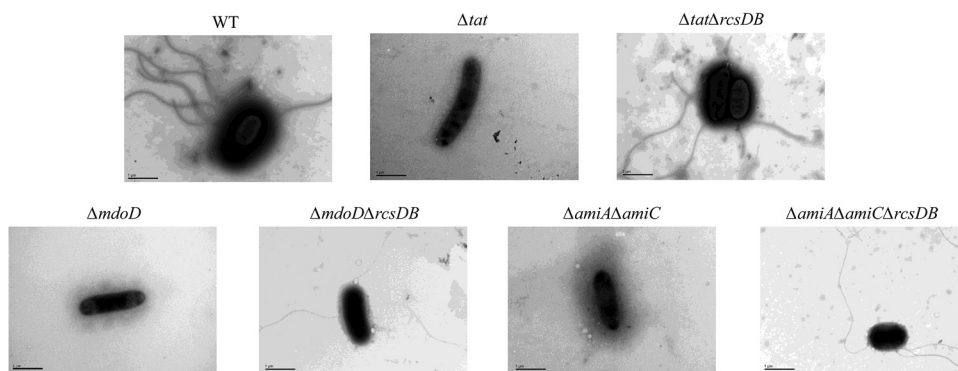


FIG 5 Transmission electron microscopy analysis of flagella. Cells of each indicated strain were streaked on an LB agar plate at 37°C for 12 h. A single colony was picked and resuspended in 200 μ L of ultrapure water, which was left to stand for 2 h. Then, 10 μ L of the bacterial suspension was placed on the grid followed by fixing with 2% phosphotungstic acid staining solution and was imaged using a transmission electron microscope (H-7650; Hitachi, Japan). The scale bar is 1 μ m.

The Rcs system was activated when the Tat system was disrupted. Previous studies have shown that the Rcs system is the negative regulator of the master transcription regulator of flagellar biosynthesis *flhDC* (18). The loss of motility could be attributed to activation of the Rcs system in the Δ *tat* strain, which downregulated the expression of the flagellar biosynthesis genes. To verify whether the Rcs system was activated when the Tat system was disrupted, we compared the expression of the genes that have been reported to be regulated by the Rcs system between the WT and the Δ *tat* strain, including *flhDC* (18), *rcnB* (40), *tssB* (20), *motB* (40), and *modA* (40). As shown in Fig. 6, the expression of *rcnB*, and *tssB* was significantly upregulated in the Δ *tat* strain compared with the WT strain. In comparison, the expression of *flhD*, *modA*, and *motB* was significantly downregulated in the Δ *tat* strain, as they have been shown to be negatively regulated by the Rcs system (40). Thus, the data indicate that the Rcs system was activated when the Tat system was disrupted.

DISCUSSION

Flagellum-mediated motility is critical for the virulence of several bacterial pathogens in which flagella function at various stages of infection. In enteropathogenic *E. coli* (EPEC), flagella promote the adhesion of bacteria to epithelial cells (41). In avian pathogenic *E. coli* (APEC) and Shiga toxin-producing *E. coli* (STEC), flagella, although not directly involved in adhesion, play important roles in invasion (42–44). Flagella have also been demonstrated to be important for the initial interaction with surfaces, which is critical for the formation of biofilms (45). Moreover, flagella can be recognized by the Toll-like receptor 5, which elicits host immune response, and bacterial pathogens have evolved strategies, such as

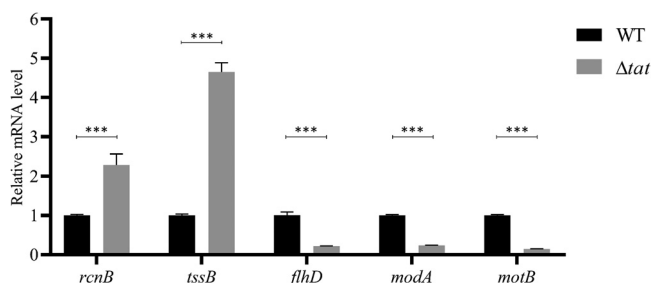


FIG 6 RT-qPCR analysis of the Rcs regulons. Total RNA was extracted from cells of each indicated strain grown to the mid-log phase. Genomic DNA was removed, and cDNA was synthesized and was used as the template for qPCR with a QuantStudio 6 Flex fluorescence quantitative PCR instrument. The expression level of the tested gene was calculated using the $2^{-\Delta\Delta CT}$ method and normalized to the housekeeping gene *gapA*. Data are displayed as the geometric mean \pm SEM. Statistical significance between the two groups was analyzed using Student's *t* test. ***, $P < 0.001$.

flagellar expression control, flagellin sequence variations, and flagellin modification, to avoid or evade such immune clearance to establish infection (46). Recently, the Tat system has been reported to play an important role in the pathogenesis of several bacteria (47–49). Interestingly, the compromised motility phenotype has been constantly observed when the Tat system is disrupted in a variety of bacteria, including *E. coli* (26), *Salmonella* (27), *P. aeruginosa* (50), and *Yersinia* (51). However, so far, the underlying mechanism of how the Tat system is linked to bacterial motility remains unclear.

To understand how the Tat system affects motility, we first compared the mRNA profile between the WT and the Δtat strain. Our data show that a substantial number of genes undergo differential expression, suggesting an important role of the Tat system in the physiology of ExPEC. The results show that the expression of capsular biosynthesis genes and stress response systems is increased in the Δtat strain (Table 1). This is consistent with the findings in a previous report (52). A possible explanation could be that the deletion of the Tat system causes outer membrane defects, which may result in the activation of the stress response systems. Among these envelope stress response systems, the Rcs system has been revealed to positively regulate the expression of capsular polysaccharide biosynthesis (53), and the activation of the Rcs system by the Tat system disruption has been implicated in the previous transcriptomics study (52). In addition, several toxin-antitoxin (TA) systems also showed differential expression in the Δtat strain (Table 1). Among them, *ghoT/S* showed a drastic upregulation upon Tat deletion, which has been reported to function under stress conditions by reducing metabolism, a possible survival strategy when confronting stresses (54). However, how the Tat system influences these TA systems needs further investigation. The downregulated genes include a substantial amount of flagellar biosynthesis genes, which corresponds with the compromised motility phenotype. This is consistent with a previous study showing that the deletion of the Tat system abolished the synthesis of flagellin in *E. coli* O157:H7 (26). However, it was not the case in *E. coli* MC4100, a commensal K-12 strain (52). Whether this difference is attributed to pathotypes remains unclear.

In *E. coli*, over 30 proteins have been predicted or verified to be transported by the Tat system (8). However, none of them has been revealed to be directly involved in flagellar biosynthesis. To reveal the link between the Tat system and flagellar biosynthesis, we perform a motility phenotype screening with the Tat substrate-related mutants, which identified three Tat substrate proteins, AmiA, AmiC, and MdoD, that are responsible for the loss of motility of the Δtat strain. Deletion of the Tat-dependent amidases AmiA and AmiC simultaneously has been previously shown to cause motility defects in both *E. coli* and *Salmonella* (25, 55). We for the first time report that another Tat substrate, MdoD (also known as OpgD), is related to bacterial motility. MdoD is involved in osmoregulated periplasmic glucan (OPG) biosynthesis in which deletion of MdoD affects the glucose backbone structures of periplasmic glucans (56). It has also been reported previously that defects in periplasmic glucan synthesis cause motility defects (36). The osmoregulated periplasmic glucans play important roles in coping with environmental stresses (37, 57). Defects in periplasmic glucans have been reported to induce envelope stress (58, 59). There are several envelope stress response systems that exist in *E. coli* to cope with envelope stresses (60), among which the Rcs system has been reported to be a negative regulator of *flhDC*, the master regulator of bacterial flagellar biosynthesis (13, 18). Our result that the disruption of the Rcs system restores the motility of the $\Delta mdoD$ strain further demonstrates an important role of Rcs in mediating the motility defects.

It should be noted that the motility was only partially restored for $\Delta tat\Delta rcsDB$ and $\Delta amiA\Delta amiC\Delta rcsDB$, suggesting that other factors than the Rcs system may also be involved in the disruption of the motility. AmiA and AmiC are two Tat-exported *N*-acetylmuramoyl-L-alanine amidases functioning in septum cleavage during cell division (61–63). Moreover, the inactivation of AmiA and AmiC is reported to compromise outer membrane integrity (35). Therefore, peptidoglycan synthesis and outer membrane integrity may be the other factors affecting the motility of the *tat* mutant.

Conclusions. In conclusion, we show that disruption of the Tat system abolishes motility of extraintestinal pathogenic *E. coli* and interferes with the expression of a

TABLE 3 Bacterial strains and plasmids used in this study

Name	Description	Reference or source
Strains		
ExPEC PCN033	A virulent clinical strain isolated from diseased pig, wild type	72
<i>E. coli</i> χ 7213	A diaminopimelic acid autotrophic <i>E. coli</i> strain used for transconjugation	73
Δ <i>tat</i>	As ExPEC PCN033, <i>tatABC</i> deleted	25
$C\Delta$ <i>tat</i>	Δ <i>tat</i> strain expressing <i>tatABC</i> from a plasmid	
Δ <i>modD</i>	As ExPEC PCN033, <i>modD</i> deleted	
Δ <i>amiA</i>	As ExPEC PCN033, <i>amiA</i> deleted	
Δ <i>amiC</i>	As ExPEC PCN033, <i>amiC</i> deleted	
Δ <i>efeOB</i>	As ExPEC PCN033, <i>efeOB</i> deleted	
Δ <i>suffl</i>	As ExPEC PCN033, <i>suffl</i> deleted	
Δ <i>mepK</i>	As ExPEC PCN033, <i>mepK</i> (previously known as <i>ycbK</i>) deleted	
Δ <i>fhuD</i>	As ExPEC PCN033, <i>fhuD</i> deleted	
Δ <i>moaA</i>	As ExPEC PCN033, <i>moaA</i> deleted	
Δ <i>nrfC</i>	As ExPEC PCN033, <i>nrfC</i> deleted	
Δ <i>hybOA</i>	As ExPEC PCN033, <i>hybOA</i> deleted	
Δ <i>yagT</i>	As ExPEC PCN033, <i>yagT</i> deleted	
Δ <i>yahJ</i>	As ExPEC PCN033, <i>yahJ</i> deleted	
Δ <i>hyaA</i>	As ExPEC PCN033, <i>hyaA</i> deleted	
Δ <i>fdoG</i>	As ExPEC PCN033, <i>fdoG</i> deleted	
Δ <i>wacM</i>	As ExPEC PCN033, <i>wacM</i> deleted	
Δ <i>cueO</i>	As ExPEC PCN033, <i>cueO</i> deleted	
Δ <i>napG</i>	As ExPEC PCN033, <i>napG</i> deleted	
Δ <i>ydhT</i>	As ExPEC PCN033, <i>ydhT</i> deleted	
Δ <i>ydhX</i>	As ExPEC PCN033, <i>ydhX</i> deleted	
Δ <i>fdnG</i>	As ExPEC PCN033, <i>fdnG</i> deleted	
Δ <i>amiA</i> Δ <i>amiC</i>	As ExPEC PCN033, <i>amiA</i> and <i>amiC</i> deleted	
Δ <i>rcsDB</i>	As ExPEC PCN033, <i>rcsDB</i> deleted	This study
Δ <i>tat</i> Δ <i>rcsDB</i>	As Δ <i>tat</i> , <i>rcsDB</i> deleted	This study
Δ <i>mdoD</i> Δ <i>rcsDB</i>	As Δ <i>mdoD</i> , <i>rcsDB</i> deleted	This study
Δ <i>amiA</i> Δ <i>amiC</i> Δ <i>rcsDB</i>	As Δ <i>amiA</i> Δ <i>amiC</i> , <i>rcsDB</i> deleted	
Δ <i>tat</i> Δ <i>cpxAR</i>	As Δ <i>tat</i> , <i>cpxAR</i> deleted	This study
Plasmids		
pRE112	The plasmid used in mutant construction	Lab stock
pHSG396- <i>Apra</i>	The plasmid used for in <i>trans</i> protein expression in ExPEC	This study
pHSG396- <i>Apra</i> - <i>MdoD</i>	As pHSG396- <i>Apra</i> , a DNA fragment containing a <i>tat</i> promoter followed by the coding sequence of <i>mdoD</i> followed by insertion between <i>Xba</i> I and <i>Eco</i> RI	This study
pHSG396- <i>Apra</i> - <i>MdoD</i> ^{RR-KK}	As pHSG396- <i>Apra</i> - <i>MdoD</i> , expressing the variant <i>MdoD</i> , where the R3 and R4 residues were both replaced with a lysine	This study
pHSG396- <i>Apra</i> - <i>RcsDB</i>	As pHSG396- <i>Apra</i> , a DNA fragment containing a <i>tat</i> promoter followed by the coding sequence of <i>rcsDB</i> inserted between <i>Xba</i> I and <i>Eco</i> RI	This study
pHSG396- <i>Apra</i> - <i>AmiA</i> / <i>AmiC</i>	As pHSG396- <i>Apra</i> , a DNA fragment containing the coding sequence of <i>rcsDB</i> followed by a <i>tat</i> promoter inserted between <i>kp</i> nI and <i>Sac</i> I	This study
pRE112- <i>rcsDB</i>	As pRE112, a DNA fragment containing the upstream 1,000 bp and downstream 1,000 bp of <i>rcsDB</i> inserted between <i>kp</i> nI and <i>Sac</i> I	This study
pRE112- <i>cpxAR</i>	As pRE112, a DNA fragment containing the upstream 1,000 bp and downstream 1,000 bp of <i>cpxAR</i> inserted between <i>kp</i> nI and <i>Sac</i> I	This study

large number of genes, among which, genes involved in flagellar biosynthesis are significantly affected. Tat substrate proteins MdoD, AmiA, and AmiC are identified that are related to the loss of motility. The Rcs system is then demonstrated to play an important role in mediating the loss of motility of the *tat* mutant. Our study for the first time reveals the underlying link between the Tat system and bacterial motility.

MATERIALS AND METHODS

Strains and plasmid construction. The strains and plasmids used in this study are all listed in Table 3. All *E. coli* strains except *E. coli* χ 7213 were grown in lysogeny broth (LB) medium or on LB agar plates at 37°C. *E. coli* strain χ 7213 was cultured in lysogeny broth (LB) medium supplemented with 50 μ g/mL of diaminopimelic acid (DAP). The DNA sequences of the primers used in this study are listed in Table S2. The gene deletion strains were constructed according to our previous report (25). Briefly, the pRE112 plasmid

containing the homologous arms flanking the target gene to be deleted was used to transform *E. coli* χ 7213 competent cells, which was used as the donor strain for transconjugation. The single exchanged strain was then confirmed by PCR after transconjugation and was incubated on 10% sucrose-containing LB to counterselect the double exchanged strain. The mutant strain was then verified by PCR. To *in trans* express the Tat substrate proteins in the mutant strains, pHSG396-Apra derivative plasmids were used in which the DNA fragment containing the corresponding coding sequence following a constitutive promoter was inserted into the multiple cloning site. The pHSG396-Apra plasmid was constructed by inserting an apramycin resistance cassette at the NcoI site within the chloramphenicol resistance cassette.

mRNA-seq. The ExPEC PCN033 and Δ *tat* strains were subcultured from overnight-grown cultures into fresh LB and grown to the mid-log phase at 37°C with shaking. The cells were harvested and washed with normal saline followed by total RNA extraction using a HiPure bacterial RNA kit (Magen, China) according to the manufacturer's instructions. RNA quantitation was performed using a Qubit 3.0 device (Thermo Fisher Scientific, Massachusetts, USA). Whole mRNA-seq libraries were constructed by Guangdong Magigene Biotechnology Co., Ltd. (Guangzhou, China), using NEBNext Ultra directional RNA library prep kit for Illumina (New England Biolabs, Massachusetts, USA) following the manufacturer's recommendations. Briefly, the bacterial 16S rRNA in the total RNA samples were depleted using a Ribo-off rRNA depletion kit (bacteria) (Vazyme, Nanjing, China). Fragmentation was carried out using the RNA first-strand synthesis module (New England Biolabs). The first-strand cDNA was synthesized using a random hexamer primer and M-MuLV reverse transcriptase (New England Biolabs). When synthesizing the second strand of cDNA, a chain-specific library was constructed by replacing dTTP with dUTP to greatly improve the accuracy of the results. The remaining overhangs were converted into blunt ends via exonuclease/polymerase activities. After adenylation of the 3' ends of DNA fragments, a NEBNext adaptor with a hairpin loop structure was ligated to prepare for hybridization. To select cDNA fragments of preferentially 150 to ~200 bp in length, the fragments were selected with SpeedBead magnetic carboxylate modified particles (Global Life Sciences Solutions Operations, Buckinghamshire, UK). Then, PCR was performed with Phusion high-fidelity DNA polymerase, universal PCR primers, and index (X) primer. Lastly, PCR products were purified with SpeedBead magnetic carboxylate modified particles, and library insert size was assessed on the Qsep400 high-throughput nucleic acid protein analysis system (Houze Biological Technology Co., Hangzhou, China). The clustering of the index-coded samples was performed on a cBot cluster generation system. After cluster generation, the library was sequenced on an Illumina NovaSeq 6000 platform, and 150-bp paired-end reads were generated.

mRNA-seq data analysis. The raw RNA-seq data in FASTQ format were processed using Trimmomatic (v0.36) to acquire the clean data (clean reads) (64). Clean reads were mapped to NCBI Rfam databases to remove the rRNA sequences with Bowtie 2 (v2.33) (65). The remaining mRNA sequences were mapped to the reference genome with HISAT 2 (v2.1.0) (66). HTSeq-count (v0.9.1) was used to obtain the read count and function information of each gene according to the result of the mapping (67). To compare the expression level of genes, the fragments per kilobase per million (FPKM) of each gene was calculated. Differentially expressed genes were analyzed using edgeR (v3.16.5) (68). The resulting *P* value was adjusted using Benjamini and Hochberg's approach for controlling the false-discovery rate. Genes with an FDR of ≤ 0.05 and $|\log_2(\text{fold change})| \geq 1$ were taken as differentially expressed genes. To do KEGG pathway enrichment, the differentially expressed genes were assigned a K number using the BlastKOALA tool (69). The K numbers were then used for pathway enrichment by using KEGG Mapper (70). The COG enrichment was performed with the EggNOG v5.0 database (71).

Motility assay. *E. coli* cells were subcultured 1:100 from overnight-grown cultures in LB and grown at 37°C with shaking to the mid-log phase. Then, 5 μ L of the bacterial culture was spotted onto the swimming plate (tryptone, 10 g/L; yeast, 5 g/L; NaCl, 10 g/L; agar, 0.2%), which was dried at room temperature for 5 min followed by incubation at 37°C for 7 h.

Transmission electronic microscopy. Cells of each indicated strain were streaked on an LB agar plate at 37°C for 12 h. A single colony was picked and resuspended in 200 μ L of ultrapure water which was left to stand for 2 h. Then, 10 μ L of the bacterial suspension was placed on the grid followed by fix with 2% phosphotungstic acid staining solution and was imaged using a transmission electron microscope (H-7650; Hitachi, Japan).

Real-time quantitative PCR. Total RNA was extracted using the RNA isolation kit (Tianmo Biotech, China). The purity and degradation of the RNA were analyzed by measuring the absorbance and agarose gel electrophoresis. HiScript Q select RT SuperMix (+gDNA wiper) (Vazyme, China) was used to remove residual genomic DNA and synthesize cDNA according to the manufacturer's instructions. The cDNA was used as the template for qPCR using the TB Green premix *Ex Taq II* kit (TaKaRa Biomedical Technology, Beijing, China) according to the manufacturer's instructions with a QuantStudio 6 Flex fluorescence quantitative PCR instrument. The expression level of the tested gene was calculated using the $2^{-\Delta\Delta CT}$ method and normalized to the housekeeping gene *gapA*.

Western blotting. To detect flagellin production, cells of each indicated strain were subcultured 1:100 from overnight-grown cultures into LB and grown to the mid-log phase at 37°C with shaking. The culture was centrifuged, and the same amount of culture supernatant was collected and concentrated by ultracentrifugation. The same number of bacterial cells were harvested, resuspended in phosphate-buffered saline (PBS), and lysed by sonication, and these were the whole-cell samples. The samples were normalized and separated on 10% SDS-PAGE and were then transferred to polyvinylidene difluoride (PVDF) membranes and probed with anti-FliC antibody (catalog [cat.] no. ab93713; Abcam, Shanghai, China).

Data availability. Sequence data have been submitted to the NCBI GEO database, and the accession number is [GSE181969](https://www.ncbi.nlm.nih.gov/geo/query/acc.cgi?acc=GSE181969).

SUPPLEMENTAL MATERIAL

Supplemental material is available online only.

SUPPLEMENTAL FILE 1, PDF file, 0.1 MB.

SUPPLEMENTAL FILE 2, XLS file, 0.1 MB.

ACKNOWLEDGMENTS

This work was supported by the National Key Research and Development Program of China (2021YFD1800401) and the National Natural Science Foundation of China (31802211).

We declare no conflict of interest.

REFERENCES

- Tseng TT, Tyler BM, Setubal JC. 2009. Protein secretion systems in bacterial-host associations, and their description in the Gene Ontology. *BMC Microbiol* 9:52. <https://doi.org/10.1186/1471-2180-9-52>.
- Costa TR, Felisberto-Rodrigues C, Meir A, Prevost MS, Redzej A, Trokter M, Waksman G. 2015. Secretion systems in Gram-negative bacteria: structural and mechanistic insights. *Nat Rev Microbiol* 13:343–359. <https://doi.org/10.1038/nrmicro3456>.
- Rapisarda C, Tassinari M, Gubellini F, Fronzes R. 2018. Using cryo-EM to investigate bacterial secretion systems. *Annu Rev Microbiol* 72:231–254. <https://doi.org/10.1146/annurev-micro-090817-062702>.
- Palmer T, Berks BC. 2012. The twin-arginine translocation (Tat) protein export pathway. *Nat Rev Microbiol* 10:483–496. <https://doi.org/10.1038/nrmicro2814>.
- DeLisa MP, Tullman D, Georgiou G. 2003. Folding quality control in the export of proteins by the bacterial twin-arginine translocation pathway. *Proc Natl Acad Sci U S A* 100:6115–6120. <https://doi.org/10.1073/pnas.0937838100>.
- Berks BC. 1996. A common export pathway for proteins binding complex redox cofactors? *Mol Microbiol* 22:393–404. <https://doi.org/10.1046/j.1365-2958.1996.00114.x>.
- Berks BC, Palmer T, Sargent F. 2003. The Tat protein translocation pathway and its role in microbial physiology. *Adv Microb Physiol* 47:187–254. [https://doi.org/10.1016/s0065-2911\(03\)47004-5](https://doi.org/10.1016/s0065-2911(03)47004-5).
- Palmer T, Sargent F, Berks BC. 2010. The Tat protein export pathway. *EcoSal Plus* 4. <https://doi.org/10.1128/ecosalplus.4.3.2>.
- De Buck E, Lammertyn E, Anne J. 2008. The importance of the twin-arginine translocation pathway for bacterial virulence. *Trends Microbiol* 16:442–453. <https://doi.org/10.1016/j.tim.2008.06.004>.
- Benoit SL, Maier RJ. 2014. Twin-arginine translocation system in *Helicobacter pylori*: TatC, but not TatB, is essential for viability. *mBio* 5:e01016-13. <https://doi.org/10.1128/mBio.01016-13>.
- McDonough JA, Hacker KE, Flores AR, Pavelka MS, Jr, Braunstein M. 2005. The twin-arginine translocation pathway of *Mycobacterium smegmatis* is functional and required for the export of mycobacterial beta-lactamases. *J Bacteriol* 187:7667–7679. <https://doi.org/10.1128/JB.187.22.7667-7679.2005>.
- Josenshans C, Suerbaum S. 2002. The role of motility as a virulence factor in bacteria. *Int J Med Microbiol* 291:605–614. <https://doi.org/10.1078/1438-4221-00173>.
- Meng J, Young G, Chen J. 2021. The Rcs system in *Enterobacteriaceae*: envelope stress responses and virulence regulation. *Front Microbiol* 12:627104. <https://doi.org/10.3389/fmicb.2021.627104>.
- Shimizu T, Ichimura K, Noda M. 2016. The surface sensor NlpE of enterohemorrhagic *Escherichia coli* contributes to regulation of the type iii secretion system and flagella by the Cpx response to adhesion. *Infect Immun* 84:537–549. <https://doi.org/10.1128/IAI.00881-15>.
- Osterman IA, Dikhtyar YY, Bogdanov AA, Dontsova OA, Sergiev PV. 2015. Regulation of flagellar gene expression in bacteria. *Biochemistry (Mosc)* 80:1447–1456. <https://doi.org/10.1134/S000629791511005X>.
- Fitzgerald DM, Bonocora RP, Wade JT. 2014. Comprehensive mapping of the *Escherichia coli* flagellar regulatory network. *PLoS Genet* 10:e1004649. <https://doi.org/10.1371/journal.pgen.1004649>.
- Wall E, Majdalan N, Gottesman S. 2018. The complex Rcs regulatory cascade. *Annu Rev Microbiol* 72:111–139. <https://doi.org/10.1146/annurev-micro-090817-062640>.
- Francez-Charlot A, Laugel B, Van Gemert A, Dubarry N, Wiorowski F, Castanie-Cornet MP, Gutierrez C, Cam K. 2003. RcsCDB His-Asp phosphorelay system negatively regulates the *flhDC* operon in *Escherichia coli*. *Mol Microbiol* 49:823–832. <https://doi.org/10.1046/j.1365-2958.2003.03601.x>.
- Spöring I, Felgner S, Preuß M, Eckweiler D, Rohde M, Häussler S, Weiss S, Erhardt M. 2018. Regulation of flagellum biosynthesis in response to cell envelope stress in *Salmonella enterica* serovar Typhimurium. *mBio* 9:e00736-17. <https://doi.org/10.1128/mBio.00736-17>.
- Hu L, Yu F, Liu M, Chen J, Zong B, Zhang Y, Chen T, Wang C, Zhang T, Zhang J, Zhu Y, Wang X, Chen H, Tan C. 2021. RcsB-dependent regulation of type VI secretion system in porcine extra-intestinal pathogenic *Escherichia coli*. *Gene* 768:145289. <https://doi.org/10.1016/j.gene.2020.145289>.
- Jozwick AKS, LaPatra SE, Graf J, Welch TJ. 2019. Flagellar regulation mediated by the Rcs pathway is required for virulence in the fish pathogen *Yersinia ruckeri*. *Fish Shellfish Immunol* 91:306–314. <https://doi.org/10.1016/j.fsi.2019.05.036>.
- Biran D, Ron EZ. 2018. Extraintestinal pathogenic *Escherichia coli*. *Curr Top Microbiol Immunol* 416:149–161. https://doi.org/10.1007/82_2018_108.
- Liu C, Zheng H, Yang M, Xu Z, Wang X, Wei L, Tang B, Liu F, Zhang Y, Ding Y, Tang X, Wu B, Johnson TJ, Chen H, Tan C. 2015. Genome analysis and *in vivo* virulence of porcine extraintestinal pathogenic *Escherichia coli* strain PCN033. *BMC Genomics* 16:717. <https://doi.org/10.1186/s12864-015-1890-9>.
- Vila J, Saez-Lopez E, Johnson JR, Romling U, Dobrindt U, Canton R, Giske CG, Naas T, Carattoli A, Martinez-Medina M, Bosch J, Retamar P, Rodriguez-Bano J, Baquero F, Soto SM. 2016. *Escherichia coli*: an old friend with new tidings. *FEMS Microbiol Rev* 40:437–463. <https://doi.org/10.1093/femsre/fuw005>.
- Liu J, Yin F, Liu T, Li S, Tan C, Li L, Zhou R, Huang Q. 2020. The Tat system and its dependent cell division proteins are critical for virulence of extraintestinal pathogenic *Escherichia coli*. *Virulence* 11:1279–1292. <https://doi.org/10.1080/21505594.2020.1817709>.
- Pradel N, Ye C, Livrelli V, Xu J, Joly B, Wu LF. 2003. Contribution of the twin arginine translocation system to the virulence of enterohemorrhagic *Escherichia coli* O157:H7. *Infect Immun* 71:4908–4916. <https://doi.org/10.1128/IAI.71.9.4908-4916.2003>.
- Reynolds MM, Bogomolnaya L, Guo J, Aldrich L, Bokhari D, Santiviago CA, McClelland M, Andrews-Polymenis H. 2011. Abrogation of the twin arginine transport system in *Salmonella enterica* serovar Typhimurium leads to colonization defects during infection. *PLoS One* 6:e15800. <https://doi.org/10.1371/journal.pone.0015800>.
- Yamanaka Y, Oshima T, Ishihama A, Yamamoto K. 2014. Characterization of the YdeO regulon in *Escherichia coli*. *PLoS One* 9:e111962. <https://doi.org/10.1371/journal.pone.0111962>.
- Osterman IA, Evfratov SA, Dzama MM, Pletnev PI, Kovalchuk SI, Butenko IO, Pobeguts OV, Golovina AY, Govorun VM, Bogdanov AA, Sergiev PV, Dontsova OA. 2015. A bacterial homolog YciH of eukaryotic translation initiation factor eIF1 regulates stress-related gene expression and is unlikely to be involved in translation initiation fidelity. *RNA Biol* 12:966–971. <https://doi.org/10.1080/15476286.2015.1069464>.
- Masuda N, Church GM. 2003. Regulatory network of acid resistance genes in *Escherichia coli*. *Mol Microbiol* 48:699–712. <https://doi.org/10.1046/j.1365-2958.2003.03477.x>.
- Guo Y, Li Y, Zhan W, Wood TK, Wang X. 2019. Resistance to oxidative stress by inner membrane protein ElaB is regulated by OxyR and RpoS. *Microb Biotechnol* 12:392–404. <https://doi.org/10.1111/1751-7915.13369>.
- Lee J, Hiibel SR, Reardon KF, Wood TK. 2010. Identification of stress-related proteins in *Escherichia coli* using the pollutant cis-dichloroethylene. *J Appl Microbiol* 108:2088–2102. <https://doi.org/10.1111/j.1365-2672.2009.04611.x>.
- Ito T, Uozumi N, Nakamura T, Takayama S, Matsuda N, Aiba H, Hemmi H, Yoshimura T. 2009. The implication of YggT of *Escherichia coli* in osmotic regulation. *Biosci Biotechnol Biochem* 73:2698–2704. <https://doi.org/10.1271/bbb.90558>.

34. Chen Y, Reinhardt M, Neris N, Kerns L, Mansell TJ, Jarboe LR. 2018. Lessons in membrane engineering for octanoic acid production from environmental *Escherichia coli* isolates. *Appl Environ Microbiol* 84:e01285-18. <https://doi.org/10.1128/AEM.01285-18>.
35. Ize B, Stanley NR, Buchanan G, Palmer T. 2003. Role of the *Escherichia coli* Tat pathway in outer membrane integrity. *Mol Microbiol* 48:1183–1193. <https://doi.org/10.1046/j.1365-2958.2003.03504.x>.
36. Kannan P, Dharne M, Smith A, Karns J, Bhagwat AA. 2009. Motility revertants of *opgGH* mutants of *Salmonella enterica* serovar Typhimurium remain defective in mice virulence. *Curr Microbiol* 59:641–645. <https://doi.org/10.1007/s00284-009-9486-8>.
37. Bontemps-Gallo S, Bohin JP, Lacroix JM. 2017. Osmoregulated periplasmic glucans. *EcoSal Plus* 7. <https://doi.org/10.1128/ecosalplus.ESP-0001-2017>.
38. Meng J, Huang C, Huang X, Liu D, Han B, Chen J. 2020. Osmoregulated periplasmic glucans transmit external signals through Rcs phosphorelay pathway in *Yersinia enterocolitica*. *Front Microbiol* 11:122. <https://doi.org/10.3389/fmicb.2020.00122>.
39. De Wulf P, McGuire AM, Liu X, Lin EC. 2002. Genome-wide profiling of promoter recognition by the two-component response regulator CpxR-P in *Escherichia coli*. *J Biol Chem* 277:26652–26661. <https://doi.org/10.1074/jbc.M203487200>.
40. Huesa J, Giner-Lamia J, Pucciarelli MG, Paredes-Martínez F, García-del Portillo F, Marina A, Casino P. 2021. Structure-based analyses of *Salmonella* RcsB variants unravel new features of the Rcs regulon. *Nucleic Acids Res* 49:2357–2374. <https://doi.org/10.1093/nar/gkab060>.
41. Girón JA, Torres AG, Freer E, Kaper JB. 2002. The flagella of enteropathogenic *Escherichia coli* mediate adherence to epithelial cells. *Mol Microbiol* 44:361–379. <https://doi.org/10.1046/j.1365-2958.2002.02899.x>.
42. La Ragione RM, Sayers AR, Woodward MJ. 2000. The role of fimbriae and flagella in the colonization, invasion and persistence of *Escherichia coli* O78:K80 in the day-old-chick model. *Epidemiol Infect* 124:351–363. <https://doi.org/10.1017/S0950268899004045>.
43. La Ragione RM, Cooley JA, Woodward MJ. 2000. The role of fimbriae and flagella in the adherence of avian strains of *Escherichia coli* O78:K80 to tissue culture cells and tracheal and gut explants. *J Med Microbiol* 49:327–338. <https://doi.org/10.1099/0022-1317-49-4-327>.
44. Best A, La Ragione RM, Sayers AR, Woodward MJ. 2005. Role for flagella but not intimin in the persistent infection of the gastrointestinal tissues of specific-pathogen-free chicks by Shiga toxin-negative *Escherichia coli* O157:H7. *Infect Immun* 73:1836–1846. <https://doi.org/10.1128/IAI.73.3.1836-1846.2005>.
45. Pratt LA, Kolter R. 1998. Genetic analysis of *Escherichia coli* biofilm formation: roles of flagella, motility, chemotaxis and type I pili. *Mol Microbiol* 30:285–293. <https://doi.org/10.1046/j.1365-2958.1998.01061.x>.
46. Rossez Y, Wolfson EB, Holmes A, Gally DL, Holden NJ. 2015. Bacterial flagella: twist and stick, or dodge across the kingdoms. *PLoS Pathog* 11:e1004483. <https://doi.org/10.1371/journal.ppat.1004483>.
47. Yan X, Hu S, Yang Y, Xu D, Li H, Liu W, He X, Li G, Cai W, Bu Z. 2020. The twin-arginine translocation system is important for stress resistance and virulence of *Brucella melitensis*. *Infect Immun* 88:e00389-20. <https://doi.org/10.1128/IAI.00389-20>.
48. Urrutia ÍM, Sabag A, Valenzuela C, Labra B, Álvarez SA, Santiviago CA. 2018. Contribution of the twin-arginine translocation system to the intracellular survival of *Salmonella* Typhimurium in *Dictyostelium discoideum*. *Front Microbiol* 9:3001. <https://doi.org/10.3389/fmicb.2018.03001>.
49. Avican U, Doruk T, Ostberg Y, Fahlgren A, Forsberg A. 2017. The Tat substrate SufI is critical for the ability of *Yersinia pseudotuberculosis* to cause systemic infection. *Infect Immun* 85:e00867-16. <https://doi.org/10.1128/IAI.00867-16>.
50. Ochsner UA, Snyder A, Vasil AI, Vasil ML. 2002. Effects of the twin-arginine translocase on secretion of virulence factors, stress response, and pathogenesis. *Proc Natl Acad Sci U S A* 99:8312–8317. <https://doi.org/10.1073/pnas.082238299>.
51. Lavander M, Ericsson SK, Bröms JE, Forsberg A. 2007. Twin arginine translocation in *Yersinia*. *Adv Exp Med Biol* 603:258–267. https://doi.org/10.1007/978-0-387-72124-8_23.
52. Ize B, Porcelli I, Lucchini S, Hinton JC, Berks BC, Palmer T. 2004. Novel phenotypes of *Escherichia coli* *tat* mutants revealed by global gene expression and phenotypic analysis. *J Biol Chem* 279:47543–47554. <https://doi.org/10.1074/jbc.M406910200>.
53. Navasa N, Rodríguez-Aparicio L, Ferrero M, Monteagudo-Mera A, Martínez-Blanco H. 2013. Polysialic and colanic acids metabolism in *Escherichia coli* K92 is regulated by RcsA and RcsB. *Biosci Rep* 33:e00038. <https://doi.org/10.1042/BSR20130018>.
54. Cheng HY, Soo VW, Islam S, McAnulty MJ, Benedik MJ, Wood TK. 2014. Toxin GhoT of the GhoT/GhoS toxin/antitoxin system damages the cell membrane to reduce adenosine triphosphate and to reduce growth under stress. *Environ Microbiol* 16:1741–1754. <https://doi.org/10.1111/1462-2920.12373>.
55. Fujimoto M, Goto R, Hirota R, Ito M, Haneda T, Okada N, Miki T. 2018. Tat-exported peptidoglycan amidase-dependent cell division contributes to *Salmonella* Typhimurium fitness in the inflamed gut. *PLoS Pathog* 14:e1007391. <https://doi.org/10.1371/journal.ppat.1007391>.
56. Lequette Y, Odberg-Ferragut C, Bohin JP, Lacroix JM. 2004. Identification of *mdoD*, an *mdoG* paralog which encodes a twin-arginine-dependent periplasmic protein that controls osmoregulated periplasmic glucan backbone structures. *J Bacteriol* 186:3695–3702. <https://doi.org/10.1128/JB.186.12.3695-3702.2004>.
57. Bontemps-Gallo S, Lacroix JM. 2015. New insights into the biological role of the osmoregulated periplasmic glucans in pathogenic and symbiotic bacteria. *Environ Microbiol Rep* 7:690–697. <https://doi.org/10.1111/1758-2229.12325>.
58. Bhagwat AA, Young L, Smith AD, Bhagwat M. 2017. Transcriptomic analysis of the swarm motility phenotype of *Salmonella enterica* serovar Typhimurium mutant defective in periplasmic glucan synthesis. *Curr Microbiol* 74:1005–1014. <https://doi.org/10.1007/s00284-017-1267-1>.
59. Amar A, Pezzoni M, Pizarro RA, Costa CS. 2018. New envelope stress factors involved in $\sigma(E)$ activation and conditional lethality of *rpoE* mutations in *Salmonella enterica*. *Microbiology (Reading)* 164:1293–1307. <https://doi.org/10.1099/mic.0.000701>.
60. Mitchell AM, Silhavy TJ. 2019. Envelope stress responses: balancing damage repair and toxicity. *Nat Rev Microbiol* 17:417–428. <https://doi.org/10.1038/s41579-019-0199-0>.
61. Heidrich C, Templin MF, Ursinus A, Merdanovic M, Berger J, Schwarz H, de Pedro MA, Holtje JV. 2001. Involvement of *N*-acetylmuramyl-L-alanine amidases in cell separation and antibiotic-induced autolysis of *Escherichia coli*. *Mol Microbiol* 41:167–178. <https://doi.org/10.1046/j.1365-2958.2001.02499.x>.
62. Vermassen A, Leroy S, Talon R, Provot C, Popowska M, Desvaux M. 2019. Cell wall hydrolases in bacteria: insight on the diversity of cell wall amidases, glycosidases and peptidases toward peptidoglycan. *Front Microbiol* 10:331. <https://doi.org/10.3389/fmicb.2019.00331>.
63. Vollmer W, Joris B, Charlier P, Foster S. 2008. Bacterial peptidoglycan (murein) hydrolases. *FEMS Microbiol Rev* 32:259–286. <https://doi.org/10.1111/j.1574-6976.2007.00099.x>.
64. Bolger AM, Lohse M, Usadel B. 2014. Trimmomatic: a flexible trimmer for Illumina sequence data. *Bioinformatics* 30:2114–2120. <https://doi.org/10.1093/bioinformatics/btu170>.
65. Langmead B, Salzberg SL. 2012. Fast gapped-read alignment with Bowtie 2. *Nat Methods* 9:357–359. <https://doi.org/10.1038/nmeth.1923>.
66. Kim D, Langmead B, Salzberg SL. 2015. HISAT: a fast spliced aligner with low memory requirements. *Nat Methods* 12:357–360. <https://doi.org/10.1038/nmeth.3317>.
67. Anders S, Pyl PT, Huber W. 2015. HTSeq: a Python framework for work with high-throughput sequencing data. *Bioinformatics* 31:166–169. <https://doi.org/10.1093/bioinformatics/btu638>.
68. Robinson MD, McCarthy DJ, Smyth GK. 2010. edgeR: a bioconductor package for differential expression analysis of digital gene expression data. *Bioinformatics* 26:139–140. <https://doi.org/10.1093/bioinformatics/btp616>.
69. Kanehisa M, Sato Y, Morishima K. 2016. BlastKOALA and GhostKOALA: KEGG tools for functional characterization of genome and metagenome sequences. *J Mol Biol* 428:726–731. <https://doi.org/10.1016/j.jmb.2015.11.006>.
70. Kanehisa M, Sato Y. 2020. KEGG Mapper for inferring cellular functions from protein sequences. *Protein Sci* 29:28–35. <https://doi.org/10.1002/pro.3711>.
71. Huerta-Cepas J, Szklarczyk D, Heller D, Hernández-Plaza A, Forslund SK, Cook H, Mende DR, Letunic I, Rattai T, Jensen LJ, von Mering C, Bork P. 2019. eggNOG 5.0: a hierarchical, functionally and phylogenetically annotated orthology resource based on 5090 organisms and 2502 viruses. *Nucleic Acids Res* 47:D309–D314. <https://doi.org/10.1093/nar/gky1085>.
72. Tang X, Tan C, Zhang X, Zhao Z, Xia X, Wu B, Guo A, Zhou R, Chen H. 2011. Antimicrobial resistances of extraintestinal pathogenic *Escherichia coli* isolates from swine in China. *Microb Pathog* 50:207–212. <https://doi.org/10.1016/j.micpath.2011.01.004>.
73. Roland K, Curtiss R, III, Sizemore D. 1999. Construction and evaluation of a delta *cya* delta *crp* *Salmonella* Typhimurium strain expressing avian pathogenic *Escherichia coli* O78 LPS as a vaccine to prevent airsacculitis in chickens. *Avian Dis* 43:429–441. <https://doi.org/10.2307/1592640>.